Available online at www.sciencedirect.com
ScienceDirect
International Journal of Mass Spectrometry 272 (2008) 165–171
International Journal of Mass Spectrometry
www.elsevier.com/locate/ijms

Parity alternation of linear ground-state hydrogenated cationic carbon clusters HC_n^+ ($n = 1$–10)

J. Yang [a], J.Y. Qi [a], M.D. Chen [a,*], Q.E. Zhang [a], C.T. Au [b]

[a] *State Key Laboratory of Physics Chemistry of Solid Surfaces, Department of Chemistry, Center for Theoretical Chemistry, College of Chemistry and Chemical Engineering, Xiamen University, Xiamen 361005, People's Republic of China*
[b] *Department of Chemistry, Hong Kong Baptist University, Kowloon Tong, Hong Kong, People's Republic of China*

Received 11 October 2007; received in revised form 29 November 2007; accepted 5 December 2007
Available online 14 December 2007

Abstract

Making use of molecular graphics software, we have designed numerous models of HC_n^+ ($n = 1$–10) cationic clusters, and performed geometry optimization and vibrational frequency calculation by means of the B3LYP density functional method. The linear ground-state isomers of HC_n^+ ($n = 1$–10) are found to be linear with the hydrogen atom located at one end of the carbon chain. When n is odd, the carbon chain is polyacetylene-like in configuration whereas when n is even, the carbon chain displays a polyacetylene-like structure that fades into a cumulenic-like arrangement towards the carbon end. We detected trends of odd/even alternation in electronic configuration, energy difference, ionization potential as well as in certain bond length and certain atomic charge of the linear ground-state HC_n^+ ($n = 1$–10) isomers. The results reveal that the odd-n cationic clusters are more stable than the even-n ones; they match the relative yields of HC_n^+ clusters as revealed in mass spectrometric investigations.

Keywords: Hydrogenated cationic carbon clusters; HC_n^+ clusters; H-substituted cluster; Density functional study

1. Introduction

The research on the structures and properties of small carbon clusters has a long history [1]. The possibility of designing novel materials by taking advantage of the size-dependent properties of atomic clusters has created tremendous interest among experimentalists and theoreticians. Among the atomic clusters investigated, the small carbon clusters are of special interest due to their importance in combustion and pyrolysis, in astrophysical processes, and in the formation and growth of fullerenes and nanotubes. In recent years, carbon chains and rings such as cyanopolyynes, isocyanopolyynes, methylpolyynes, methylcyanopolyynes, cumulene carbenes, and ring-chain carbenes have been identified in supersonic molecular beams by means of Fourier-transform microwave spectroscopy [2,3]. Among the carbon-chain molecules, the hydrogenated ones belong to a popular kind of species. In the past decade, Bell et al. reported the observation of long C_nH molecules in the TMC-1 dust cloud [4] and Millar described the detection of species that belong to the polyyne families in circumstellar environment of late-type carbon-rich stars (such as star IRC + 10216), and in dense and dark interstellar molecular clouds (such as TMC-1) as well as in hot molecular cores [5]. In the laboratories, polyyne compounds were generated by means of laser ablation of graphite targets and arcing across graphite electrodes in ammonia [6]. The electronic spectra of gas-phase $C_{2n+1}H$ ($n = 2$–4) radicals have been recorded by Ding et al. [7]. By means of Fourier transform microwave spectroscopy, McCarthy et al. detected the singly substituted carbon-13 isotopic species of C_3H, C_5H, C_6H, and C_7H in a supersonic molecular beam [8]. With the discovery of long-chain carbon molecules in interstellar and circumstellar environments, the H-substituted carbon clusters have received much attention. For example, Hallett et al. and Schlatholter et al. investigated the generation of H-substituted carbon clusters by means of cluster vaporization source [9] and solid C_{84} impacted by highly charged ions [10], respectively.

Due to the intriguing findings, a number of theoretical investigations on hydrogenated carbon cluster have been conducted. Raghavachari et al. studied the structures and energetics of C_1–C_3 carbocations by means of ab initio calculations with MP perturbation [11]. The geometries of $C_{2n+1}H$, $C_{2n+1}H^+$,

* Corresponding author. Tel.: +86 592 2182332; fax: +86 592 2184708.
E-mail addresses: mdchen@xmu.edu.cn, mdchen_xmu@yahoo.cn (M.D. Chen).

1387-3806/$ – see front matter © 2008 Elsevier B.V. All rights reserved.
doi:10.1016/j.ijms.2007.12.004

and various $C_{2n+1}H_2$ species ($n = 1$–3) predicted based on ab initio calculations were reported by Cooper at al. [12]. Largo and Barrientos carried out ab initio studies (at the Hartree-Fock level of the low-lying states) of the radicals and positive ions of C_2H, C_2F and C_2Cl [13]. In addition, ab initio calculations were employed to study the low-lying states of C_3H^+ by Largo-Cabrerizo et al. [14]. Botschwina studied HC_5^+ by the coupled electron pair approximation (CEPA) using a basis set of cGTOs [15]. Woon studied the linear carbon-chain C_nH ($n = 2$–7) radicals with correlation consistent valence and core-valence basis sets and the coupled cluster method RCCSD(T) [16]. By means of high level coupled cluster methods, Crawford et al. investigated the structures and energetics of C_5H isomers [17]. Using molecular orbital calculations, Blanksby et al. studied the two isomers originated from the corresponding C_5H anions [18]. Using B3LYP DFT method, Pan et al. conducted investigation on C_nH^- ($n \leq 10$) clusters [19], and using B3LYP density functional method, Zhang et al. examined the size dependence of electronic excitation energy of $C_{2n}H$ [20].

The emission of small $C_nH_m^+$ ($n = 3$–20, $m = 0$–3) clusters upon impact of highly charged Xe^{q+} ($q = 20$–44) on C_{84} surfaces was studied by means of time-of-flight secondary ion mass spectrometry [10]. According to the results, the relative yields of odd-n HC_n^+ ($n \leq 10$) clusters are higher than those of even-n ones, implying that the former are more stable than the latter. To explore the experimental observation theoretically, we conducted B3LYP density functional calculation on the HC_n^+ ($n = 1$–10) clusters. We first identified the ground-state geometry and then studied the bonding character, atomic charge, electronic configuration, energy difference, ionization potentials, and dissociation channels of them. Based on the results, we provide explanation on why the odd-n HC_n^+ ($n = 1$–10) isomers are more stable than the even-n ones. The findings are expected to elucidate the mechanism of hydrogen interaction with the small carbon clusters in terms of cluster size. The outcomes can serve as a guideline for the synthesis of similar kind of materials as well as for future theoretical studies on hydrogenated carbon clusters which are so commonly found in circumstellar environments.

2. Computational method

During the investigation, devices for molecular graphics, molecular mechanics, and quantum chemistry were used. To start, a model of a cluster was designed initially using HyperChem for Windows [21] and Desktop Molecular Modeller [22] on a PC computer. The model was optimized by MM+ molecular mechanics and semi-empirical PM3 quantum chemistry. Then, geometry optimization and calculation of vibrational frequencies were conducted using the B3LYP density functional method of Gaussian 03 package [23] with 6–311G** basis sets, i.e., Becke's 3-parameter nonlocal exchange functional with the correlation functional of Lee–Yang–Parr [24,25]. It has been pointed out that geometries computed with more expensive basis sets do not necessarily lead to results of better accuracy [26]. The single point energy calculations following the optimization were performed using the larger 6–311+G** basis set (i.e., B3LYP/6–311+G**//B3LYP/6–311G**). Because the change of zero point energy (ZPE) could only be affected minutely by the quality of the employed method, all energies were calculated with ZPE correction at the B3LYP/6–311G** level. The optimized models were again displayed using HyperChem for Windows. The data of partial charges and bond orders were explored with Gaussian Natural Bond Orbital (NBO). All of the calculations were carried out on the servers of SGI.

3. Results and discussion

3.1. Geometry configuration

The possible structures of the carbon clusters are many, and the ground-state isomers of the heteroatom(s)-doped carbon clusters may adopt a large variety of configurations. The linear configurations terminated by the heteroatom(s) are rather popular among the most stable isomers, e.g., BeC_n^- ($n = 1$–8) [27]. For the boron-doped carbon clusters C_nB ($n = 4$–10) [28] and beryllium-doped carbon dianion clusters C_nBe^{2-} ($n = 4$–14) [29], the linear configurations with the boron and beryllium atom located inside the carbon chain are the most stable. For C_nH^- ($n \leq 10$) clusters, the configurations with a bent C_n chain terminated at one end by the hydrogen atom are the most favorable in energy [19]. In the cases of CsC_7^- and CsC_9^-, isomers with a "lightly embracing" structure have been suggested to be the most stable [30].

At the beginning of our investigation, we designed the initial structures of HC_n^+ ($n = 1$–10) according to chemical understandings. In order to reduce the chance of having the ground-state structures wrongly determined, it is necessary to consider a huge number of geometrical structures. We studied isomers of linear, bent-chain, branch, cyclic and bicyclic structures. Optimization of each cluster was performed by starting with different spin multiplicities and initial structures, and through the exploration of potential energy surface, the geometry corresponding to the global minimum was located. After the optimization process, the total energies were compared for the identification of ground-state isomers. For models with imaginary vibrational frequencies and/or of higher energies, they were discarded.

Seven major categories of HC_n^+ ($n = 1$–10) structures are displayed in Fig. 1. Belong to category 1a are isomers of linear structures, the H atom is located at one end of the C_n chain. The isomers of category 1b are "Y" shape with the H atom located at the end of one of the branches. The isomers of category 1c are with the H atom bonded to a C atom which is connected to two carbon branches. In category 1d are isomers with the H atom bonded to a C atom of a C_n ring. The isomers of category 1e show a carbon ring with a C atom bonded to a $-C_xH$ chain. Belong to category 1f are isomers with a $-C_x$ chain and the H atom bonded to two separate C atoms of a C_{n-x} ring. The isomers of category 1g show a C_{n-x-1} ring with one of the ring atoms bonded to a $-C_xC$ chain; the H atom is bonded to one of the non-terminating carbon atoms of the $-C_xC$ chain. After comparing the total energies, the linear ground-state geometries of HC_n^+ ($n = 1$–10) are identified to be those of category 1a.

A hydrogen atom has only one electron available for interaction and cannot be incorporated as an internal part of a chain or

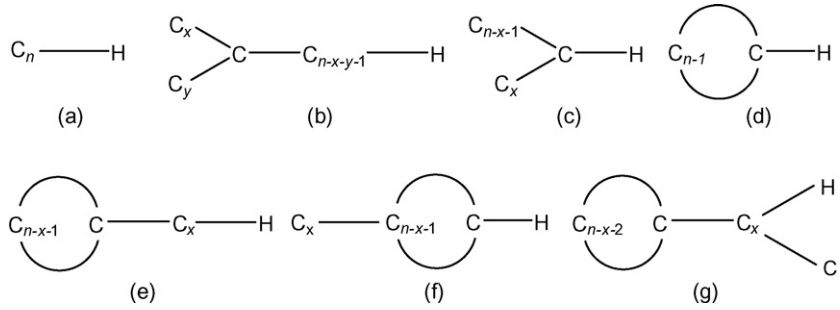

Fig. 1. Seven main categories of HC_n^+ ($n = 1$–10) structures (x, y denote numbers of carbon atom(s)).

ring. This is the reason why the H atom is always located at the end of a linear chain. If the hydrogen atom were initially attached to a non-terminating atom of a carbon chain, it would end up at one end of the chain after geometry optimization. Nonetheless, the hydrogen atom may attach to one of the carbon atoms of a ring or a branch structure, and the isomers are higher in total energy compared to the corresponding linear counterparts. The same can be observed in the case of neutral C_nH clusters. Pan et al. optimized four isomers of C_7H, and found that the ground-state isomer is linear in structure and the isomers with the hydrogen atom attached to a carbon atom of a ring structure are higher in total energy [19]. Crawford et al. optimized seven isomers of C_5H by means of high level coupled cluster methods, the linear structures were determined as ground-state isomers [17].

3.2. Bonding character

Displayed in Fig. 2 are the bond lengths and NBO charges of the linear ground-state HC_n^+ ($n = 1$–10) clusters. One can

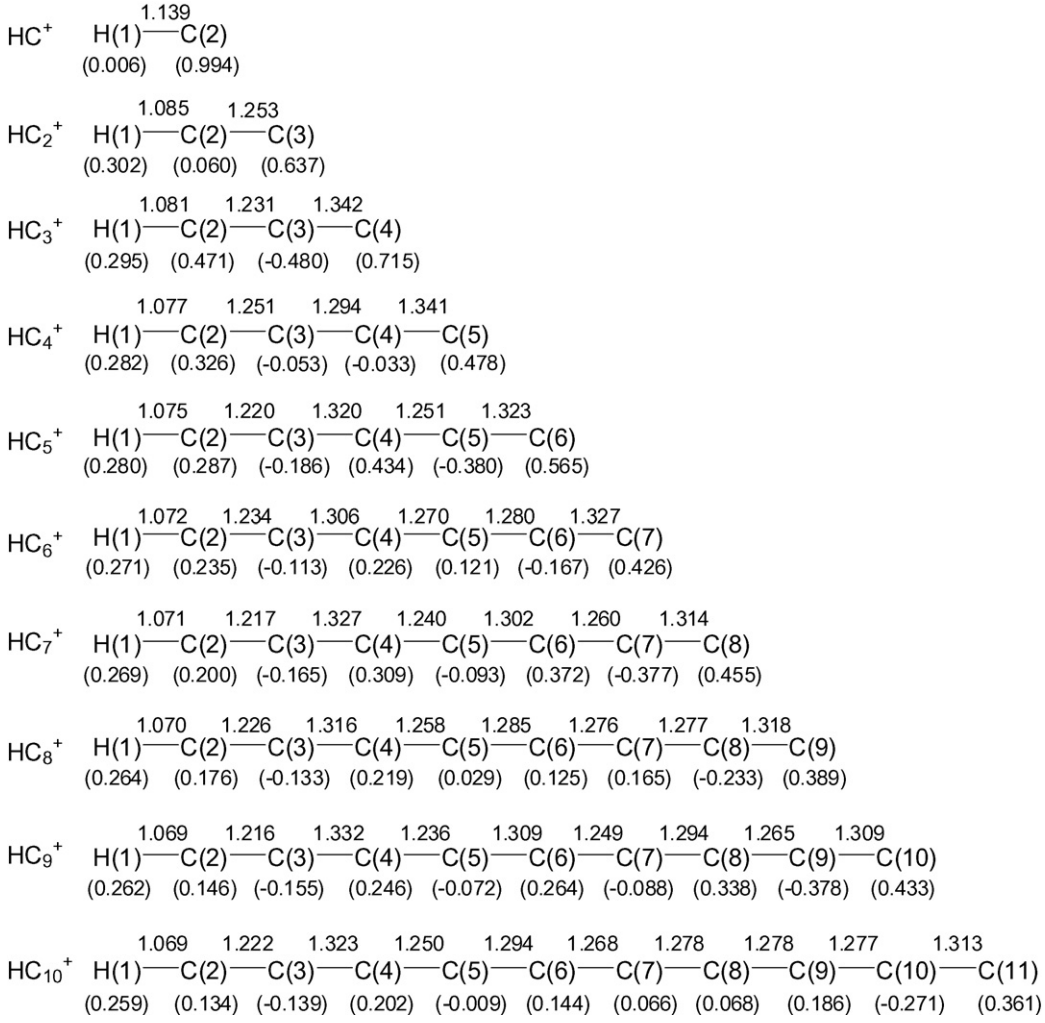

Fig. 2. Bond lengths (Å) and NBO charges (in parentheses) of the linear ground-state HC_n^+ ($n = 1$–10) clusters.

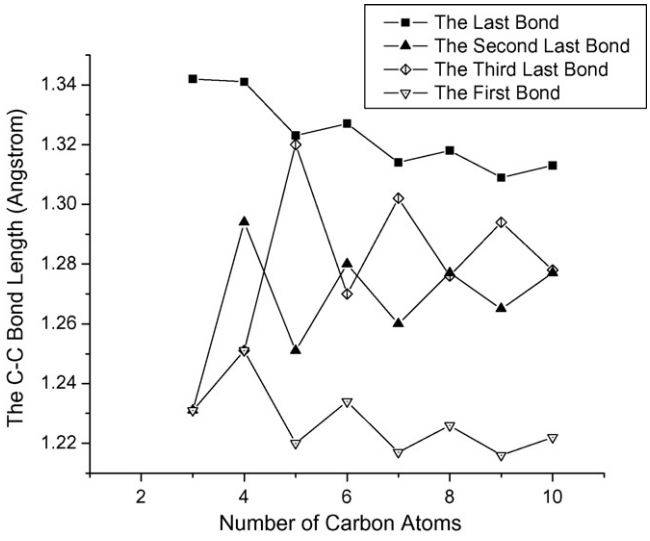

Fig. 3. Length (Å) of the first, the last, the second last, and the third last C–C bonds of the linear ground-state HC_n^+ (n = 3–10) clusters vs. n.

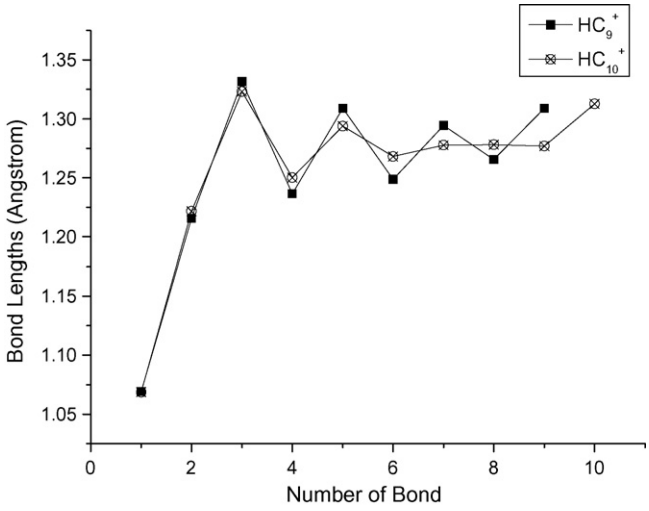

Fig. 4. Bond lengths (in Å) of the linear ground-state HC_9^+ and HC_{10}^+ clusters vs. the number of bond (as counted from the left side of chains in Fig. 2).

see that the H–C lengths are within the 1.069–1.139 Å range, exhibiting essentially the characteristics of single bond. Shown in Fig. 3 are the plots of the bond lengths of the first, the last, the second last, and the third last C–C bonds (as counted from the left) of the linear ground-state HC_n^+ (n = 3–10) clusters versus the number of carbon atoms (n). For the bond lengths of the first and the second last C–C bonds, one can see patterns of distinct odd/even alternation: The C–C bond lengths of the even-n clusters are longer than those of the neighboring odd-n ones. One can also see that the alternation magnitude of the former is smaller than that of the latter, and the C–C bond lengths decrease with a rise in n. Comparing to that of the first and the second last C–C bonds, the alternation magnitude in bond length of the last C–C bonds is relatively small. As for the bond lengths of the third last C–C bonds, they show distinct odd/even alternation but with parity inverse to those of the first, the last and the second last C–C bonds. It has been pointed out that the bonding of linear carbon chains can be either cumulene- or polyacetylene-like [31]. Along the chains of the linear ground-state HC_n^+ (n = 3–10) isomers, the length of the C–C bonds shows an alternate short/long pattern. When n is odd, the C–C bonds display a typical polyacetylene-like character, i.e., a series of alternate single and triple bonds. When n is even, the pattern of short/long alternation of C–C bond lengths fades out gradually from the H end towards the carbon end of the chain, and the C–C bonds close to the carbon end tend to even out in length, showing some sort of cumulenic character (i.e., with consecutive double bonds). As an illustration, depicted in Fig. 4 are the bond lengths of the linear ground-state HC_9^+ and HC_{10}^+ clusters versus the number of bond (as counted from the left in Fig. 2, e.g., the H–C bond length is plotted against "1" and so on). The curve of the HC_9^+ with polyacetylene-like carbon chain displays the pattern of short/long alternation. As for HC_{10}^+, the carbon chain is polyacetylene-like along the side close to the H terminus but cumulene-like along the other side. The results of NBO bond order analysis confirm the above bonding characteristics. When n is odd, the carbon chains are clearly characterized by a series of alternate single and triple bond, and the clusters adopt a structure that shows characteristics of polyacetylene-like clusters.

Also displayed in Fig. 2 are the NBO atomic charges (values in parentheses underneath the atoms) of the linear ground-state HC_n^+ (n = 1–10) clusters. Shown in Fig. 5 is a plot of the charges on the last, the second last, and the third last carbon atom of the linear ground-state HC_n^+ (n = 1–10) clusters versus n. The levels of positive charges on the last C atoms are relatively higher than those on the third last and the second last C atoms. The value of positive charges (in the range of 0.361–0.994) on the last C atoms shows a pattern of odd/even alternation. That of an odd-n cluster is larger than that of the neighboring even-n ones, and the charges decrease with a rise in n. The third last C atoms accommodate positive charges in the range of 0.186–0.471 for n = 3, 5–9 and negative charges of −0.053 for n = 4, showing odd/even pattern similar to that of the last C atoms but with larger alternation magnitude. The charge of the second carbon atoms are mostly

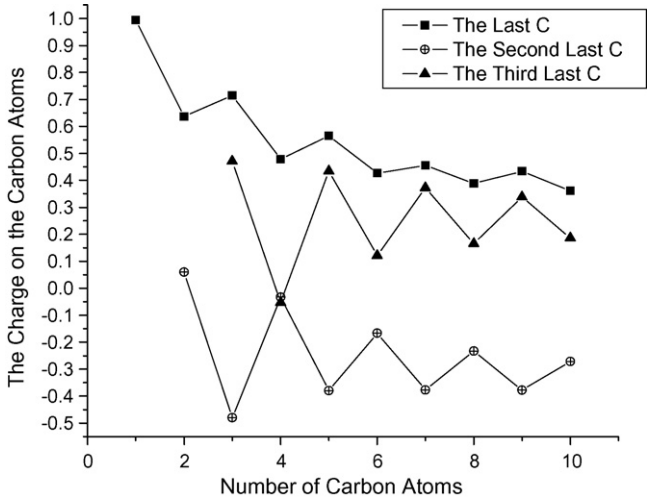

Fig. 5. The charge on the last, the second last, and the third last carbon atoms of the linear ground-state HC_n^+ (n = 1–10) clusters vs. n.

Table 1
Valence orbital configurations of the linear ground-state HC_n^+ (n = 1–10) clusters

Isomers	Configuration
HC^+	(core) $\sigma^2\sigma^2\sigma^2$
HC_2^+	(core) $\sigma^2\sigma^2\sigma^1\pi^3$
HC_3^+	(core) $\sigma^2\sigma^2\sigma^2\sigma^2\pi^4$
HC_4^+	(core) $\sigma^2\sigma^2\sigma^2\sigma^2\pi^4\sigma^2\pi^2$
HC_5^+	(core) $\sigma^2\sigma^2\sigma^2\sigma^2\sigma^2\pi^4\sigma^2\pi^4$
HC_6^+	(core) $\sigma^2\sigma^2\sigma^2\sigma^2\sigma^2\sigma^2\pi^4\pi^4\sigma^2\pi^2$
HC_7^+	(core) $\sigma^2\sigma^2\sigma^2\sigma^2\sigma^2\sigma^2\sigma^2\pi^4\pi^4\sigma^2\pi^4$
HC_8^+	(core) $\sigma^2\sigma^2\sigma^2\sigma^2\sigma^2\sigma^2\sigma^2\sigma^2\pi^4\pi^4\pi^4\sigma^2\pi^2$
HC_9^+	(core) $\sigma^2\sigma^2\sigma^2\sigma^2\sigma^2\sigma^2\sigma^2\sigma^2\sigma^2\pi^4\pi^4\pi^4\sigma^2\pi^4$
HC_{10}^+	(core) $\sigma^2\sigma^2\sigma^2\sigma^2\sigma^2\sigma^2\sigma^2\sigma^2\sigma^2\sigma^2\pi^4\pi^4\pi^4\pi^4\sigma^2\pi^2$

Table 2
Electronic state, total energy (a.u.), energy difference ΔE_n (a.u.), and ionization potential (IP) (a.u.) of the linear ground-state HC_n^+ (n = 1–10) clusters

Clusters	State	Total energy	ΔE_n	IP
CH^+	$^1\Sigma^+$	−38.08324		0.404500
C_2H^+	$^3\Pi$	−76.19188	−38.10864	0.423096
C_3H^+	$^1\Sigma^+$	−114.34993	−38.15805	0.343409
C_4H^+	$^3\Sigma^-$	−152.42361	−38.07368	0.362870
C_5H^+	$^1\Sigma^+$	−190.55507	−38.13147	0.317294
C_6H^+	$^3\Sigma^-$	−228.62811	−38.07304	0.332689
C_7H^+	$^1\Sigma^+$	−266.74536	−38.11724	0.301443
C_8H^+	$^3\Sigma^-$	−304.81945	−38.07409	0.313545
C_9H^+	$^1\Sigma^+$	−342.92992	−38.11047	0.290273
$C_{10}H^+$	$^3\Sigma^-$	−381.00545	−38.07553	0.299946

negative (in the range of −0.271 to 0.060), showing obvious odd/even alternation inverse to those of the last and third last atoms, and the charge decreases with a rise in n.

3.3. Electronic configuration

Shown in Table 1 are the configurations of valence orbitals for the linear ground-state HC_n^+ (n = 1–10) clusters.

The electronic configurations can be depicted as (except for HC^+ and HC_2^+)

$$(\text{core})1\sigma^2 \ldots 1\pi^4 \ldots (n+1)\sigma^2 \left(\frac{n-1}{2}\right)\pi^4 \quad n \text{ is odd}$$

$$(\text{core})1\sigma^2 \ldots 1\pi^4 \ldots (n+1)\sigma^2 \left(\frac{n}{2}\right)\pi^2 \quad n \text{ is even}$$

The linear ground-state HC_n^+ (n = 3–10) clusters possess $4n$ valance electrons, among which are $2n-2$ π-electrons and $2n+2$ σ-electrons. Thus for odd n, the highest occupied molecular orbital (HOMO) with doubly degenerate π orbital is fully occupied. Such a situation (i.e., with fully filled π-orbital) is energetically more favorable than that with a half-filled shell. The linear ground-state HC_n^+ (n = 3–10) alternates between $^1\Sigma^+$ (odd n) and $^3\Sigma^-$ (even n) electronic states. This arises from the fact that all MOs with π-symmetry are doubly degenerate. When n is odd, the addition of an extra carbon atom would result in having two more electrons included in the π-system, and the accommodation of these two electrons in a π-orbital would lead to a triplet state.

3.4. Energy differences

The energy difference which is defined as the difference between the total energies of the adjacent clusters can be used to evaluate the relative stability of the clusters of various sizes. For the cationic clusters, the energy difference is determined as

$$\Delta E_n = E(HC_n{}^+) - E(HC_{n-1}{}^+)$$

Listed in Table 2 are the electronic state, total energy, energy difference (ΔE_n), and ionization potential (IP) of the linear ground-state HC_n^+ (n = 1–10) clusters acquired using zero point energy correction. In the case of triplet-state HC_n^+ (n = 1–10) isomers. The spin contamination $\langle S^2\rangle$ value (before annihilation of the contaminants) stays within the 2.02–2.11 range, and such a small deviation should not have severe effect on our results.

Displayed in Fig. 6 is the variation of energy differences (ΔE_n) of the linear ground-state HC_n^+ (n = 1–10) clusters versus n. One can see that the odd-n clusters are lower than the even-n clusters in ΔE_n values. The results illustrate that the clusters with odd n are more stable than those with even n.

3.5. Ionization potentials

Ionization potentials (IP, adiabatic) are computed as the energy difference between the optimized cationic and neutral clusters ($E_{\text{optimized cation}} - E_{\text{optimized neutral}}$). A lower IP means that less energy is needed to remove an electron from the neutral molecule, and the generation of the corresponding cationic isomer is more readily done. Shown in Fig. 7 is the IP variation curve of linear ground-state HC_n^+ (n = 1–10) versus n. One can see that the IP values of HC_n^+ with odd n are lower than those of the neighboring even-n ones, and the IP values decrease with a rise in n. This implies that compared to the cases of even n, it is easier to remove an electron from a neighboring odd-n HC_n. The pattern of odd/even alternation reiterates that the clusters with odd n are more stable than those with even n. Such odd/even

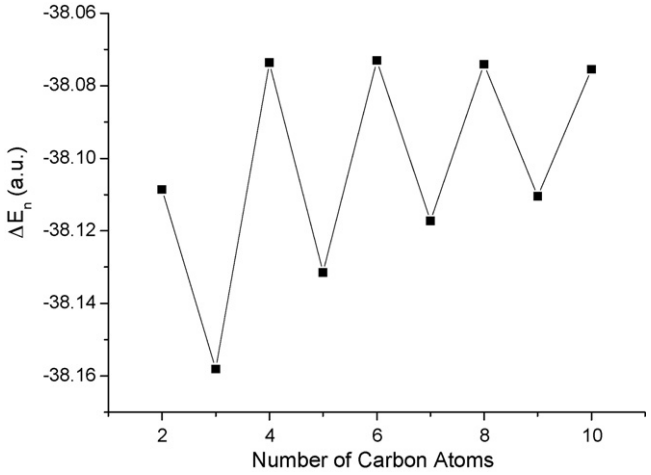

Fig. 6. Energy differences ΔE_n (a.u.) of the linear ground-state HC_n^+ (n = 1–10) clusters (as shown in Table 2) vs. the number of carbon atoms.

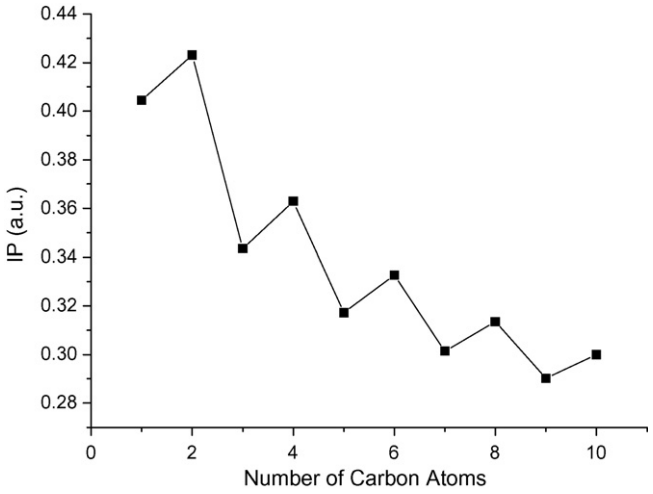

Fig. 7. Electron affinity IP (a.u.) of the linear ground-state HC_n^+ (n = 1–10) clusters (as shown in Table 2) vs. n.

alternation of IP and ΔE_n is in consistency with the experimental observation that the odd-n clusters are higher in abundance than the even-n ones [10]. Since the IP of the odd-n clusters are obviously lower than that of the even-n clusters and the ΔE_n of the odd-n clusters are lower than that of even-n clusters, it is envisaged that the odd-n clusters are more stable and less susceptible to fragmentation.

Proton affinity (PA) of a molecule can be defined as the energy released when a proton (H^+) is added to the molecule, and is computed as the difference in energy between the molecule and the as-generated cation [26]. The PA of C_n can thus be related to the energy of C_nH^+ quantitatively as PA = E (C_n) − E (C_nH^+). The PA of linear C_n (n = 2–9) clusters are 0.25137, 0.30078, 0.21641, 0.27420, 0.21577, 0.25998, 0.21682, and 0.25320 a.u., respectively. Fig. 8 is a plot of the PA values versus n. With H^+ added to a terminating C atom, the formation of the C–H bond would result in having the positive charge incorporated into the π system. As depicted in Fig. 8, there is a nearly linear rise of PA values versus n. It is apparent that with n increases, there is enhanced stability of the HC_n^+ clusters due to the wider spread of the positive charge in the enlarged π system.

3.6. Dissociation channels

Despite there is only one hydrogen atom located at one end of the carbon chains, the possible dissociation channels of HC_n^+ (n = 1–10) could still be complicated. We have no attempt to characterize the reaction pathways and transition states for fragmentation in this work. Our evaluation of the relative stability of the clusters in terms of fragmentation energy is based on hypothetical pathways only. The six dissociation channels are divided into two groups: reactions (1)–(3) with C, C_2, and C_3 generation and reactions (4)–(6) with H, HC, and HC_2 generation, respectively.

$$C_nH^+ \rightarrow C_{n-1}H^+ + C \quad (1)$$

$$C_nH^+ \rightarrow C_{n-2}H^+ + C_2 \quad (2)$$

$$C_nH^+ \rightarrow C_{n-3}H^+ + C_3 \quad (3)$$

$$C_nH^+ \rightarrow C_n{}^+ + H \quad (4)$$

$$C_nH^+ \rightarrow C_{n-1}{}^+ + CH \quad (5)$$

$$C_nH^+ \rightarrow C_{n-2}{}^+ + C_2H \quad (6)$$

The fragmentation energies versus n are depicted in Fig. 9. Fragmentation energies related to reaction (1) with the release of one carbon atom exhibits distinct odd/even alternation and the dissociation energies with odd n are always larger than those with even n. The results reiterate that the linear ground-state HC_n^+ (n = 1–10) with odd n are relatively more stable; the ejection of a single carbon atom will cause an inversion in parity of the clusters and the more stable odd-n clusters requires more energy for fragmentation than the less stable even-n clusters. In reaction (2), the loss of a C_2 fragment does not involve significant change in parity of the parent cationic clusters, and the alternation effect is much less apparent than that of reaction (1). The energy curve

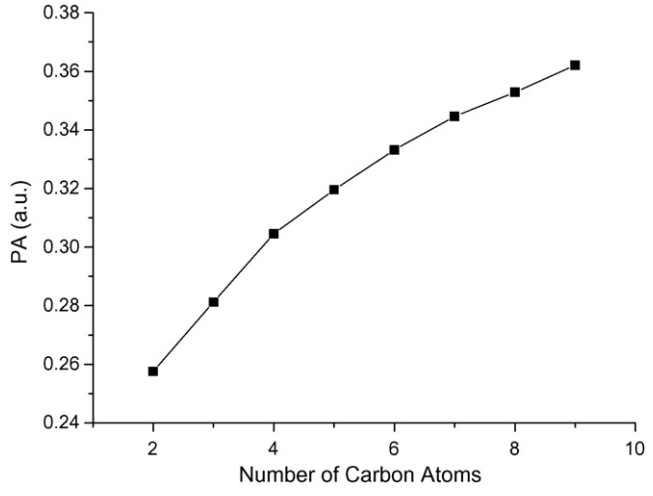

Fig. 8. Proton affinities PA (a.u.) of linear ground-state C_n (n = 2–9) clusters vs. n.

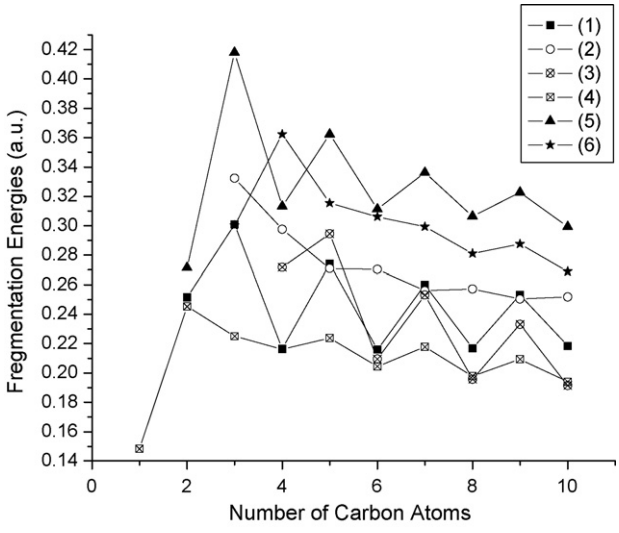

Fig. 9. Fragmentation energy (a.u.) vs. the number of carbon atoms.

of reaction (3) shows an odd/even trend similar to that of reaction (1). The dissociation energies of reaction (3) are smaller than those of reactions (1) and (2), plausibly due to the special structural stability of the C_3 fragment as previously pointed out by Rao et al. [32]. The dissociation energy of reactions (4)–(6) which involve the loss of H, CH, and C_2H, respectively, exhibit similar trends of odd/even alternation. Reaction (4) with the loss of a hydrogen fragment shows a slight change in parity when n is bigger than 3, the dissociation energy are the smallest and the loss of a hydrogen atom is likely to be the dominant dissociation pathway. Compared to reaction (4) that involves the breaking of the H–C bond, reaction (5) needs more energy because it involves the breaking of the C–CH bond. The dissociation energies of reaction (5) exhibit distinct odd/even alternation with the dissociation energies of odd-n clusters always larger than those of even-n ones. The dissociation energies of reaction (6) show a trend of odd/even alternation when n is smaller than 5, and the trend becomes less apparent when n is bigger than 5. In summary, the dissociation energies of reactions (1), (3), and (5) for HC_n^+ (n = 1–10) show clear pattern of odd/even alternation: Those of the odd-n isomers are larger than those of the neighboring even-n ones.

4. Conclusion

The ground-state structures of HC_n^+ (n = 1–10) are linear with the H atom located at one end of the C_n chain. When n is odd, the bond lengths and bond orders suggest a polyacetylene-like structure along the C_n chain, whereas when n is even, the data suggest a polyacetylene-like structure that fades into a cumulenic-like arrangement towards the carbon end. The odd-n clusters are more stable than the even-n ones. The regularity of odd/even alternation are illustrated according to the properties of bond character, atomic charge, electronic configuration, energy difference, and ionization potential. The results are in concord with the relative abundance of the HC_n^+ (n = 1–10) species observed in experimental studies.

Acknowledgement

This work was supported by the National Science Foundation of China (grant 20473061, and 20533020).

References

[1] W. Weltner Jr., R.J. Van Zee, Chem. Rev. 89 (1989) 1713.
[2] P. Thaddeus, M.C. McCarthy, Spectrochim. Acta Part A 57A (2001) 757.
[3] P. Thaddeus, M.C. McCarthy, M.J. Travers, C.A. Gottlieb, W. Chen, Faraday Discuss. 109 (1998) 121.
[4] M.B. Bell, P.A. Feldman, J.K.G. Watson, M.C. McCarthy, M.J. Travers, C.A. Gottlieb, P. Thaddeus, Astrophys. J. 518 (1999) 740.
[5] T.J. Millar, Astrophys. Space Sci. Libr. 305 (2004) 17.
[6] F. Cataldo, Int. J. Astrobiol. 5 (2006) 37.
[7] H. Ding, T. Pino, F. Guthe, J.P. Maier, J. Chem. Phys. 117 (2002) 8362.
[8] M.C. McCarthy, P. Thaddeus, J. Chem. Phys. 122 (2005) 174308/1.
[9] R.P. Hallett, K.G. McKay, S.P. Balm, A.W. Allaf, H.W. Kroto, A.J. Stace, Z. Phys. D 34 (1995) 65.
[10] T. Schlatholter, M.W. Newman, T.R. Niedermayr, G.A. Machicoane, J.W. McDonald, T. Schenkel, R. Hoekstra, A.V. Hamza, Eur. Phys. J. D 12 (2000) 323.
[11] K. Raghavachari, R.A. Whiteside, J.A. Pople, P.V.R. Schleyer, J. Am. Chem. Soc. 103 (1981) 5649.
[12] D.L. Cooper, S.C. Murphy, Astrophys. J. 333 (1988) 482.
[13] A. Largo, C. Barrientos, Chem. Phys. 138 (1989) 291.
[14] A. Largo-Cabrerizo, J.R. Flores, Int. J. Quantum Chem. 36 (1989) 241.
[15] P. Botschwina, J. Chem. Phys. 95 (1991) 4360.
[16] D.E. Woon, Chem. Phys. Lett. 244 (1995) 45.
[17] T.D. Crawford, J.F. Stanton, J.C. Saeh, H.F. Schaefer III, J. Am. Chem. Soc. 121 (1999) 1902.
[18] S.J. Blanksby, S. Dua, J.H. Bowie, J. Phys. Chem. A 103 (1999) 5161.
[19] L. Pan, B.K. Rao, A.K. Gupta, G.P. Das, P. Ayyub, J. Chem. Phys. 119 (2003) 7705.
[20] C.J. Zhang, Z.X. Cao, Q.E. Zhang, Chem. Res. Chin. Univ. 19 (2003) 454.
[21] Hypercube Inc., Hyerchem Reference Manual, Waterloo, Ont., Canada, 1996.
[22] M. James, C. Crabbe, J.R. Appleyard, C.R. Lay, Desktop Molecular Modeller, Oxford University Press, Walton Street, Oxford, Great Britain, 1994.
[23] M.J. Frisch, G.W. Trucks, H.B. Schlegel, G.E. Scuseria, M.A. Robb, J.R. Cheeseman, J. Montgomery, J.A.T. Vreven, K.N. Kudin, J.C. Burant, J.M. Millam, S.S. Iyengar, J. Tomasi, V. Barone, B. Mennucci, M. Cossi, G. Scalmani, N. Rega, G.A. Petersson, H. Nakatsuji, M. Hada, M. Ehara, K. Toyota, R. Fukuda, J. Hasegawa, M. Ishida, T. Nakajima, Y. Honda, O. Kitao, H. Nakai, M. Klene, X. Li, J.E. Knox, H.P. Hratchian, J.B. Cross, V. Bakken, C. Adamo, J. Jaramillo, R. Gomperts, R.E. Stratmann, O. Yazyev, A.J. Austin, R. Cammi, C. Pomelli, J.W. Ochterski, P.Y. Ayala, K. Morokuma, G.A. Voth, P. Salvador, J.J. Dannenberg, V.G. Zakrzewski, S. Dapprich, A.D. Daniels, M.C. Strain, O. Farkas, D.K. Malick, A.D. Rabuck, K. Raghavachari, J.B. Foresman, J.V. Ortiz, Q. Cui, A.G. Baboul, S. Clifford, J. Cioslowski, B.B. Stefanov, G. Liu, A. Liashenko, P. Piskorz, I. Komaromi, R.L. Martin, D.J. Fox, T. Keith, M.A. Al-Laham, C.Y. Peng, A. Nanayakkara, M. Challacombe, P.M.W. Gill, B. Johnson, W. Chen, M.W. Wong, C. Gonzalez, J.A. Pople, Gaussian 03 (Revision D.01), Gaussian, Inc., Wallingford CT, 2004.
[24] A.D. Becke, J. Chem. Phys. 98 (1993) 5648.
[25] C. Lee, W. Yang, R.G. Parr, Phys. Rev. B: Condens. Matter 37 (1988) 785.
[26] J.B. Foresman, Æ. Frisch, Exploring Chemistry with Electronic Structure Methods, Gaussian Inc., Pittsburgh, PA, 1996.
[27] M.D. Chen, X.B. Li, J. Yang, Q.E. Zhang, C.T. Au, Int. J. Mass Spectrom. 253 (2006) 30.
[28] K. Chuchev, J.J. BelBruno, J. Phys. Chem. A 108 (2004) 5226.
[29] M.D. Chen, X.B. Li, J. Yang, Q.E. Zhang, C.T. Au, J. Phys. Chem. A 110 (2006) 4502.
[30] A. Dreuw, L.S. Cederbaum, J. Chem. Phys. 111 (1999) 1467.
[31] A. Van Orden, R.J. Saykally, Chem. Rev. 98 (1998) 2313.
[32] B.K. Rao, S.N. Khanna, P. Jena, Solid State Commun. 58 (1986) 53.